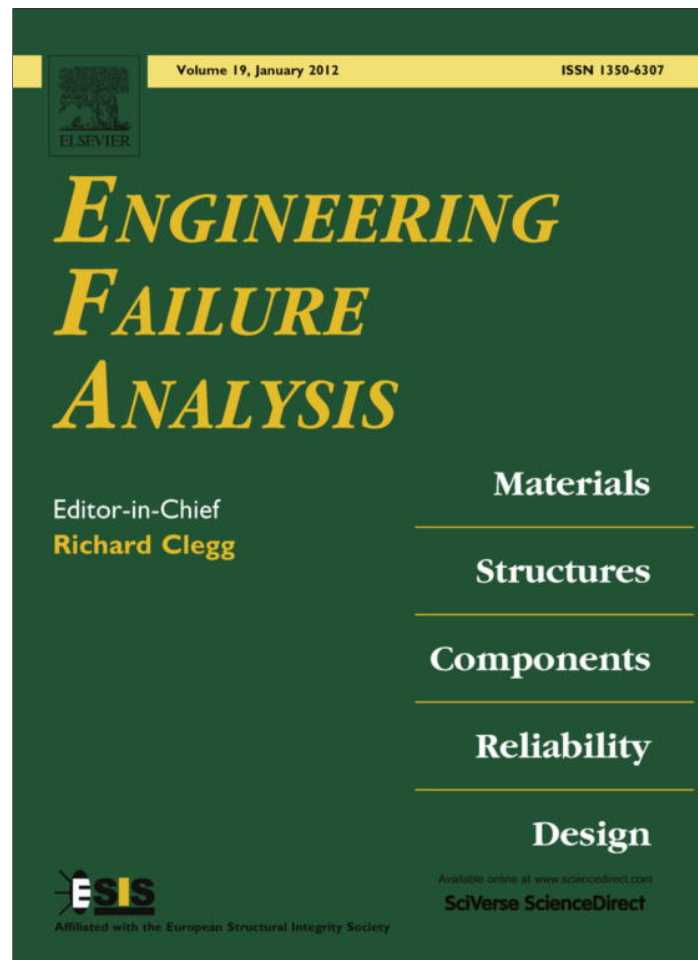


Provided for non-commercial research and education use.
Not for reproduction, distribution or commercial use.



(This is a sample cover image for this issue. The actual cover is not yet available at this time.)

This article appeared in a journal published by Elsevier. The attached copy is furnished to the author for internal non-commercial research and education use, including for instruction at the authors institution and sharing with colleagues.

Other uses, including reproduction and distribution, or selling or licensing copies, or posting to personal, institutional or third party websites are prohibited.

In most cases authors are permitted to post their version of the article (e.g. in Word or Tex form) to their personal website or institutional repository. Authors requiring further information regarding Elsevier's archiving and manuscript policies are encouraged to visit:

<http://www.elsevier.com/copyright>

Contents lists available at [SciVerse ScienceDirect](#)

Engineering Failure Analysis

journal homepage: www.elsevier.com/locate/engfailanal

Failure analysis of the oil transport spiral welded pipe

Meng-Bin Lin^{a,b}, Kewei Gao^{b,*}, Chaur-Jeng Wang^a, Alex A. Volinsky^c^a Department of Mechanical Engineering, National Taiwan University of Science and Technology, Taipei, Taiwan^b Department of Materials Physics and Chemistry, University of Science and Technology Beijing, Beijing 10083, China^c Department of Mechanical Engineering, University of South Florida, Tampa, FL 33620, USA

ARTICLE INFO

Article history:

Received 22 March 2011

Received in revised form 11 May 2012

Accepted 14 May 2012

Available online 19 May 2012

Keywords:

Failure analysis

Failure mechanism

Inclusions

Welded pipe

ABSTRACT

The spiral welded pipe for oil transport failed catastrophically fracturing along the spiral welding line. The failure was in the base metal close to the heat-affected zone. Passive inclusions in the rolled metal are responsible for the pipe failure. Microstructure examination and Charpy-V notch tests reveal that the crack follows the oxide inclusions and is associated with their distribution, since the base metal toughness is insufficient to retard cracking. Improvement of the steel purity is suggested to prevent future pipe failures. Improving the welding technique to reduce the residual stress acting on the base metal also decreases the risk of pipe failure.

© 2012 Elsevier Ltd. All rights reserved.

1. Introduction

Spiral welded pipes are extensively used in the petroleum industry for oil and gas transport. They are made from a coiled hot-rolled steel strip with a single continuous helical weld from end to end [1,2]. This article describes examples of the spiral welded pipe failures. The spiral welded pipe for transporting oil was made from API 5L X52 steel. The pipe diameter is 720 mm with 8–10 mm wall thickness. The weld joint is a double V type. The outside and the inside welds were made by submerged arc welding with 60° welding angle. The pipe maximum working pressure is 3.8 MPa with 30–60 °C working temperature range. Although the working pressure never exceeded the maximum working pressure limitation, parts of the pipe broke catastrophically along the spiral weld (Fig. 1a).

This study was commissioned to identify factors causing pipe failure. The microstructure and microhardness of the weld metal, weld junction, heat-affected zone and base metal were considered. The fracture mechanism was identified, highlighting factors that contributed to the spiral welded pipe failure. Finally, recommendations were proposed to avoid this type of spiral welded pipe failure.

2. Methodology

Specimens were cut from the failed pipe (Fig. 1b), mounted with Epoxy, grinded with emery paper to 2000 grade, and polished. In order to observe the macrostructure and microstructure, specimens were etched in 95% CH₃OH + 5% HNO₃ solution for 14 s.

The Charpy V-notch (CVN) impact test [3] was conducted to evaluate the notch sensitivity and impact toughness of the spiral welded pipe (base metal). Specimens (5 × 10 × and 55 mm long) were cut parallel and perpendicular to the rolling direction in order to compare the toughness in different orientations; their corresponding positions are presented in Fig. 2.

* Corresponding author.

E-mail address: kwgao@mater.ustb.edu.cn (K. Gao).

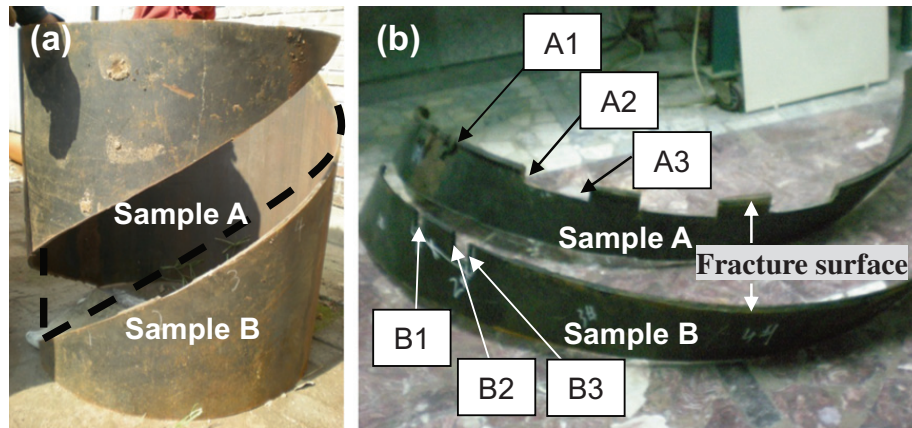


Fig. 1. (a) Fractured spiral welded pipe as received; (b) locations of analyzed specimens.

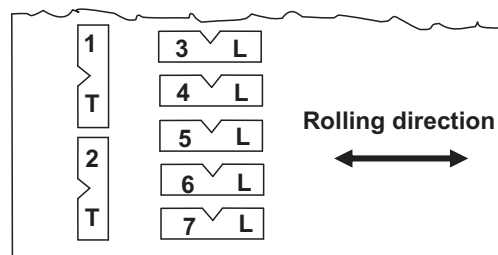


Fig. 2. Specimens for the Charpy V-notch impact test prepared in longitudinal (L) and transverse (T) orientations.

The fracture morphology and specimens' microstructure were investigated by means of optical microscopy (Leica, Germany) and scanning electron microscopy (SEM, Zeiss EVO18, Germany) equipped with energy-dispersive spectrometer (EDS). The microhardness of the welded and heat affected zones, and matrix was measured using a Vickers microhardness tester (Akashi MVK-H1, Japan).

3. Results and discussion

3.1. Failed pipe microstructure examination

Visual inspection of the etched specimens revealed that the fracture did not occur at the welding zone, but at the heat affected zone, or base metal; thus the weld was left on one fracture side, as seen in Fig. 3a and b. The spiral welded pipe microstructure is divided in three zones: welded metal, heat-affected zone (surrounding the weld), and the base metal.

In order to investigate the weld metal and the base metal compatibility, their microstructures and hardness were compared. The weld metal microstructure is lath ferrite [4] (Fig. 4a), and next to it is the heat-affected zone (HAZ). Since the heating temperature and subsequent cooling rate vary with the distance to the heat source [4,5], the heat-affected zone contains two different structures: acicular ferrite and the fine grained zone, as presented in Fig. 4b and c. Base metal exhibits fiber texture, indicating that the base metal sheets were produced by rolling (Fig. 4d). The microhardness of the weld metal, acicular ferrite zone, is HV 200, while for the fine grained zone and base metal it is HV 170. Thus, plastic deformation compatibility between weld and base metals appears suitable.

However, it was found that the base metal has low purity. Fig. 5a shows passive inclusions distributed in the base metal. A crack has nucleated at the matrix-inclusion interface (Fig. 5b). In addition, analysis by energy dispersive spectroscopy (EDS) revealed these inclusions to be iron oxide (Fig. 5b and Table 1). A number of studies [6–9] have been made on the effects of nonmetallic inclusions on the mechanical properties and fracture of alloys. Rosenfield [11] has published a thorough review of the mechanisms of initiation, growth, and coalescence of microcracks resulting from either inclusion-matrix interface separation or inclusion fracture during mechanical testing. It has been observed that the microcracks associated with inclusions can cause premature fracture and ductility. Therefore, the oxide inclusions presenting in the base metal would attribute to the pipe failure.

3.2. Failure mechanism

In order to understand the failure mechanism, fracture topography of the failed pipe should be considered. Before observing the fracture surface, the specimens were cleaned with acid pickling solution (500 mL HCl + 500 mL water + 3.5 g

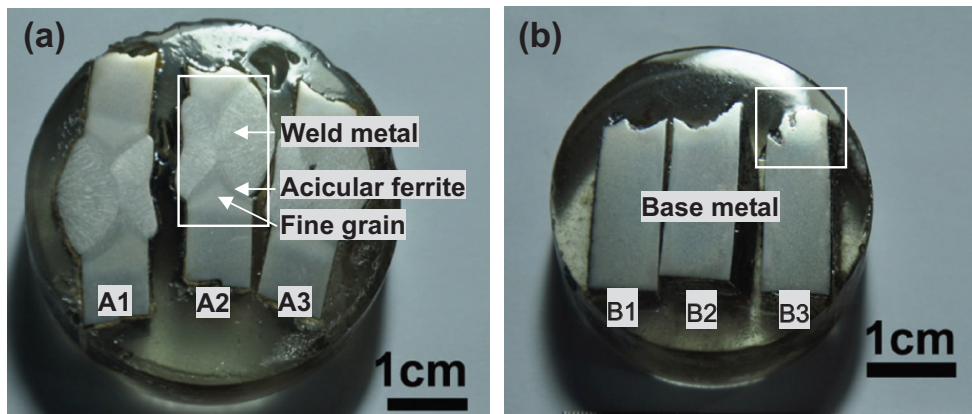


Fig. 3. Visual inspection of cross sections of fractured pipe after etching: (a) from sample A; (b) from sample B.

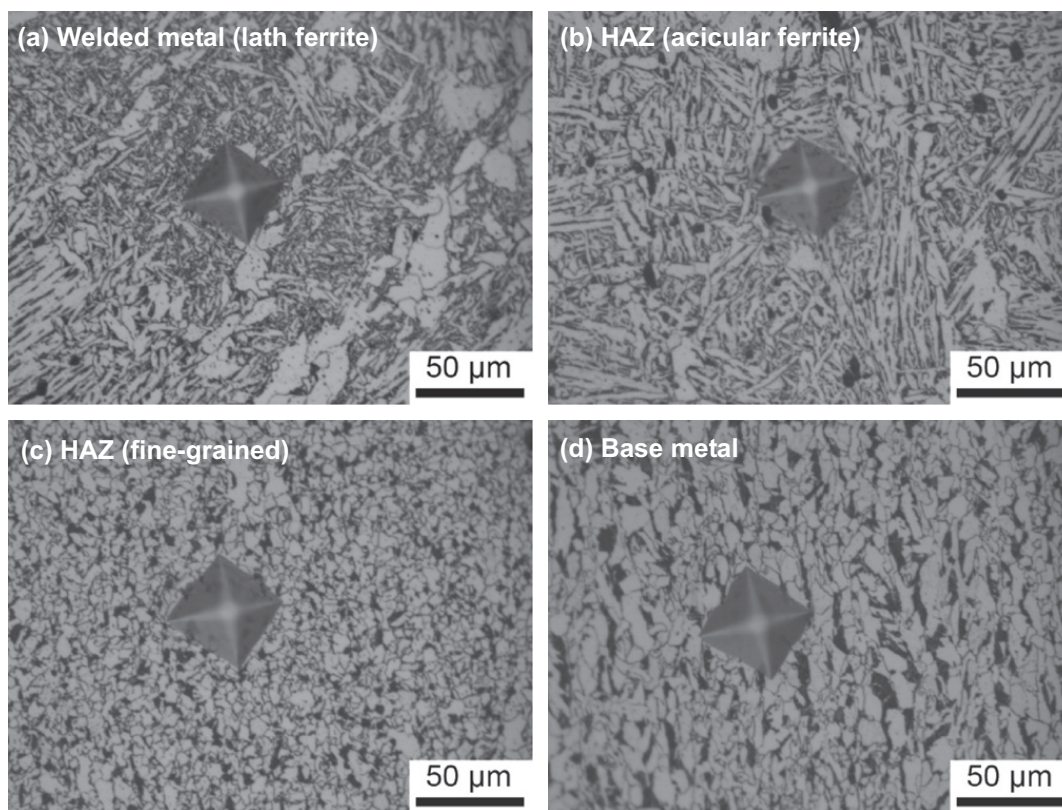


Fig. 4. Optical micrographs of cross-sections and Vickers hardness indentation of: (a) welded metal zone, lath ferrite with HV 200 hardness; (b) heat-affected zone (HAZ), acicular ferrite with HV 200 hardness; (c) fine grain ferrite with HV 170 hardness; (d) base metal with fiber texture and hardness similar to the fine-grained zone (HV 170).

hexamethylene tetramine). Cross-sectional fracture morphology was also examined, providing more information about the fracture mechanism.

SEM micrographs of the failed pipe are presented in Fig. 6a and b. Lamellar and deep groove fracture topography was observed, associated with inclusions distribution. SEM micrographs of the failed pipe cross-sections (Fig. 6c and d) contribute significantly to explanation of the pipe failure mechanism. Crack propagation is dominated by the inclusions distribution. The mechanical resistance of base metal is significantly reduced by the inclusions presence, resulting in cracks associated with inclusions. Many studies have been conducted concerning the influence of inclusions on strength and toughness reduction [6–9]. The base metal of the failed pipe is subject to significant stress concentration due to the existence of inclusions. Consequently, it is reasonable to believe that these passive inclusions are the major reason leading to pipe failure.

In order to prove that alignment of passive inclusions resulted in mechanical resistance anisotropy leading to pipe failure, the Charpy V-notch impact test (CVN, ASTM E23) was conducted. The CVN specimens were prepared with the notch in the sheet plane either parallel or perpendicular to the rolling direction (Fig. 2). The corresponding experimental data of the CVN

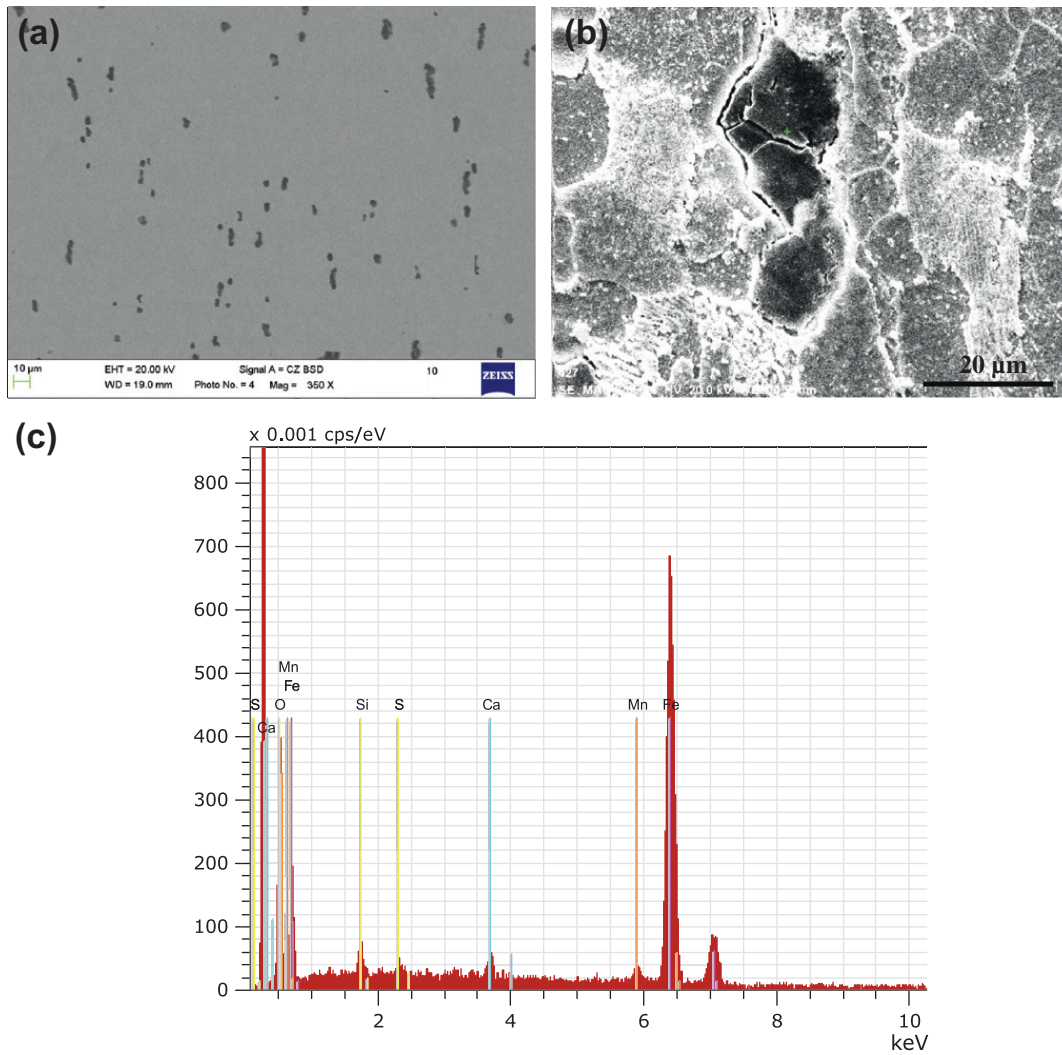


Fig. 5. (a) Distribution of inclusions in the fiber texture; (b) the oxide inclusion on the polished surface of the base metal of the pipe, (c) EDS spectrum of the oxide inclusion in (b) with, quantitative composition results shown in Table 1.

Table 1
EDS elemental analysis of the inclusions observed in Fig. 5b (at.%).

Element	Fe	O	Mn	Ca	Si	S
Inclusion	48.79	46.08	1.63	1.25	1.64	0.61

test is shown in Table 2. Longitudinally orientated specimens with respect to the rolling direction (No. 3 through No. 7) exhibited 40–44 J Charpy V-notch impact energy, while the impact energy of the perpendicular orientated samples (No. 1 and No. 2) significantly decreased to 10–12 J. SEM micrographs of perpendicular-orientated specimens (No. 1, 10 J impact energy) and longitudinally-orientated specimens (No. 4, 40 J impact energy) are shown in Fig. 7a and b. The low impact energy specimen (10 J, perpendicular orientation) exhibits deep grooves and laminate fracture topography. Ductile fracture topography in terms of dimples is associated with high 40 J impact energy for the longitudinally-oriented specimens (parallel to the rolling direction). Therefore, the CVN test revealed that due to passive inclusions aligned along the fiber texture, the base metal exhibits insufficient strength and toughness along the rolling direction. Significant cracking occurs at low stress, consequently leading to pipe failure [6].

Moreover, welding residual stress may also promote crack growth. Welding residual stress resulted from localized volume expansion. Welded metal cooling results in significant tensile stress acting on the surrounding base metal [10]. Combination of the residual stress and stress concentration promote cracks propagating along the spiral weld, finally causing catastrophic pipe failure.

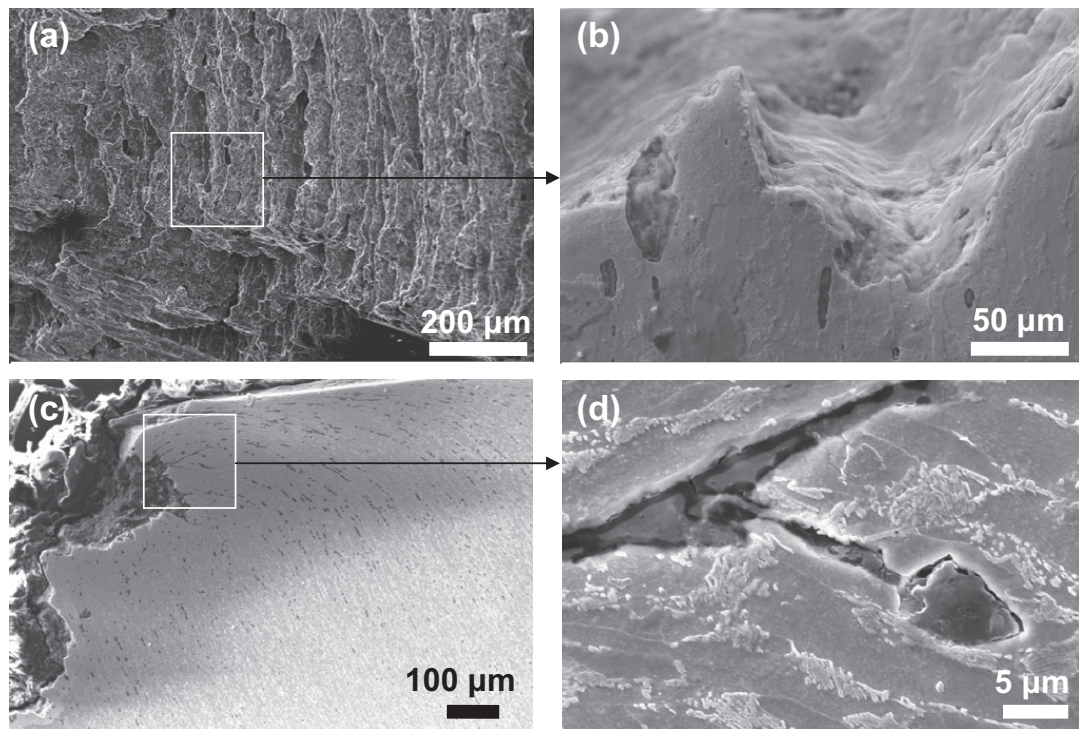


Fig. 6. SEM micrographs of the failed pipe: (a and b) fracture surface; (c and d) cross sections and material cracking associated with inclusions.

Table 2
The Charpy V-notch impact energy.

Specimen	No. 1	No. 2	No. 3	No. 4	No. 5	No. 6	No. 7
Impact energy	10 J	12 J	39 J	40 J	42 J	44 J	44 J

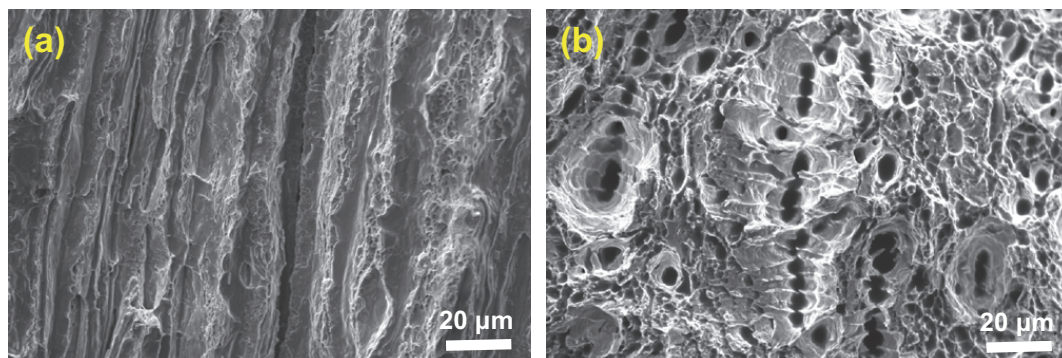


Fig. 7. The fracture morphology of the impact test specimens: (a) along the rolling direction with the Charpy V-notch impact energy of 10 J, and the fracture morphology revealing lamellar tearing; (b) perpendicular to the rolling direction with the Charpy V-notch impact energy of 39 J, and dimple fracture surface.

4. Conclusions

In this study proposed failure mechanism is summarized in Fig. 8. Significant amount of inclusions aligned along the fiber rolling texture significantly reduced the base metal mechanical resistance, resulting in propagating cracks associated with the inclusions. Finally, combination of welding residual stress and stress concentration promote crack growing easily along the spiral weld, and subsequent pipe failure.

The improvement of steel purity may offer a solution to the fracture and subsequent failure of the pipe. Besides, improving the welding technique to reduce the residual stress acting on the base metal, may also decrease the risk of pipe cracking.

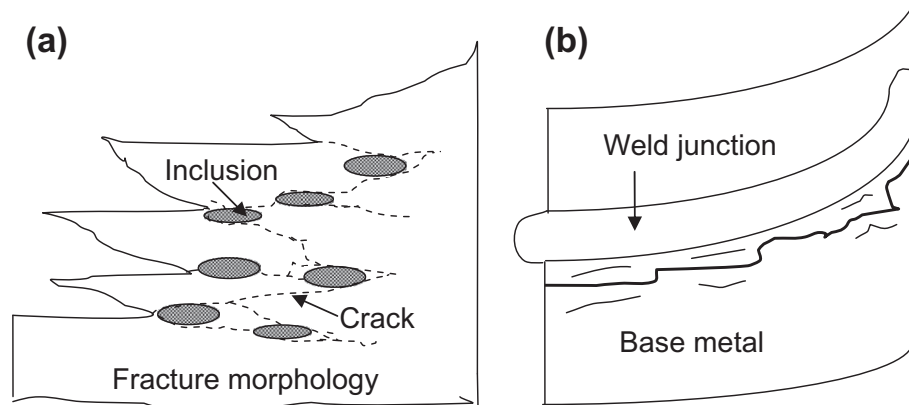


Fig. 8. Schematic of the failure mechanism: (a) crack progression through inclusions; (b) residual stress promoting material cracking and consequent pipe failure along the spiral weld.

Acknowledgements

M.B. Lin would like to acknowledge financial support from the University of Science and Technology Beijing. Alex Volinsky would like to acknowledge support from the National Science Foundation.

References

- [1] Michikiyo M, Toyofumi K, Hirofumi N, Yukio N, Toshikazu Y. High speed welding techniques for spiral pipe production. *Nippon Kokan Tech Report Overseas* 1986;46:53–60.
- [2] Pyshmintsev IYu, Pumpyanskiy DA, Kamenskiy YuO, Poznyakovskiy IN, Permyakov IL. Strengthening low carbon steels for oil and gas spiral welded pipes. In: *Proceedings of the biennial international pipeline conference*, vol. 3. Calgary, AB, Canada, 2007. p. 269–74.
- [3] ASTM E23, Standard test methods for notched bar impact testing of metallic materials, *Annual book of ASTM standards*, vol. 03.01.
- [4] Farrar RA, Harrison PL. Review acicular ferrite in carbon-manganese weld metals: an overview. *J Mater Sci* 1987;22:3812–20.
- [5] Zheng H, Ye X, Jiang L, Wang B, Liu Z, Wang G. Study on microstructure of low carbon 12% chromium stainless steel in high temperature heat-affected zone. *Mater Des* 2010;31:4836–41.
- [6] Spitzig WA. Effect of shape of sulfide inclusions on anisotropy of inclusion spacings and on directionality of ductility in hot-rolled C–Mn steels. *Metall Trans A* 1984;15:1259.
- [7] Domizzi G, Anteri G, Ovejero-García J. Influence of sulphur content and inclusion distribution on the hydrogen induced blister cracking in pressure vessel and pipeline steels. *Corrosion Sci* 2001;43:325–39.
- [8] Avdusinovic H, Gigovic A. The morphology and distribution of MnS in low carbon steel. *Metalurgija* 2005;44:151–4.
- [9] Baker TJ, Gove KB, Charles JA. Inclusion deformation and toughness anisotropy in hot-rolled steels. *Metall Technol* 1976;3:183–93.
- [10] Lee HW, Kang SW. The relationship between residual stresses and transverse weld cracks in thick steel plate. *Weld J* 2003;82:225–30.
- [11] Rosenfield AR. *Metall Rev* 1968;13:29–40.